



# Effect of Coupling Channel on Elastic Scattering for ${}^6\text{He}+{}^{208}\text{Pb}$ , ${}^7\text{Be}+{}^{58}\text{Ni}$ and ${}^7\text{Li}+{}^{59}\text{Co}$ Systems

Zainab H. Mousa<sup>1\*</sup>, Fatima M. Hussain<sup>2</sup>

## Abstract

Effects of coupling channel on elastic scattering have been studied using the nuclear potential Woods-Saxon (WS) for  ${}^6\text{He}+{}^{208}\text{Pb}$ ,  ${}^7\text{Be}+{}^{58}\text{Ni}$  and  ${}^7\text{Li}+{}^{59}\text{Co}$  systems. The Continuum-discretized coupled-channels CDCC method have been used to employed no coupled and coupled-channels (CC) calculations for unstable projectiles. Cross-sections of elastic scattering were extracted from the optical potential fits, to achieve the optimum comparability between the theoretical estimates of  $d\sigma_{el}/d\sigma_R$  and empirical values for the systems reviewed. The breakup process at near Coulomb barrier energies play essential role in the results of cross section as a function of angle and energy in addition to the distribution of the barrier.

**Key Words:** Elastic Scattering, Woods-Saxon Potential, Coupled Channels, CDCC Method.

**DOI Number:** 10.14704/nq.2022.20.2.NQ22078

**NeuroQuantology 2022; 20(2):119-123**

## Introduction

The reaction mechanisms involved in colliding both stable and unstable nuclei of near-barrier energy have been one of the principal focuses of investigation in low-energy nuclear physics. To comprehend the many mechanisms of the collision, including the main interconnections, vast experimental and theoretical attempts were conducted. On this subject, there have been a number of comprehensive review studies published (Canto *et al*, 2006; Keeley *et al*, 2007; Keeley *et al*, 2009; Back *et al*, 2014; Canto *et al*, 2015). The nucleus-nucleus interaction is an important part of understanding nucleus activities (Bass, 1980; Denisov, 2004), and it has been used to characterize nucleus-nucleus collisions (Hagino & Watanabe, 2007). The interaction energy of colliding nuclei is determined by the nucleus-nucleus potential (Satchler, 1983; Denisov & Nesterov, 2006). It's been used to calculate the cross sections of a number

of nuclear processes (Denisov, 2004). Furthermore, the nucleus-nucleus potential in deformed nucleus contact is dependent on the orientation angle of the deformed nucleus respect to the beam path (Hagino, 2007; Wong, 1973). The nucleus-nucleus potential can be described as the sum of the nuclear part  $V_N(r)$ , which is less well defined, and the coulomb part  $V_C(r)$ , which is very recognized (Denisov, 2004) due to the appropriate depiction of coulomb or Rutherford scattering (Ibrahim *et al*, 2013). The relation between the nuclear and coulomb potentials, which occur at short ranges between the surfaces of the reactant nuclei, determines the barrier height of the nucleus-nucleus collision (Denisov & Nesterov, 2006).

The nuclear potential takes place between protons and neutrons, while long-range repulsive coulomb potential occurs between protons in nuclei (Denisov & Nesterov, 2006).

**Corresponding author:** Zainab H. Mousa

**Address:** <sup>1,2</sup>Department of Physics, College of Education for Pure Science, University of Babylon, Iraq.

<sup>1</sup>E-mail: zaynab.hafiz.pure352@student.uobabylon.edu.iq

<sup>2</sup>E-mail: pure.fatima.mohammed@uobabylon.edu.iq

**Relevant conflicts of interest/financial disclosures:** The authors declare that the research was conducted in the absence of any commercial or financial relationships that could be construed as a potential conflict of interest.

**Received:** 29 December 2021 **Accepted:** 24 January 2022



The Woods-Saxon (WS) from (Berkdemir *et al*, 2005) is often used to express the nuclear interaction, which is distinguished by the depth  $V_0$ , radius  $r_0$ , and propagation  $a_0$  variables (Gasques *et al*, 2007). The concept that the surface property of nuclear potential has been studied using the WS shape of a simple exponential (Hagino *et al*, 2005) In nuclear physics, the WS potential is crucially significant because it is regarded as a realistic potential (Pahlavani *et al*, 2009). The standard value of the surface propagation coefficient, which is about 0.63 fm, has been utilized for elastic scattering values, which are essentially reactive to the surface region of the nuclear potential (Washiyama *et al*, 2006).

Halo nuclei are weakly bound exotic nuclei that display unusual states in which protons and neutrons extend beyond the nuclear drip line (Tanihata, 1996). In the recent decade, there has been a lot of interest in studying halo/ weakly bound nucleus collisions. Furthermore, considerable effects on elastic distribution and fusion were detected due to the coupling of the disintegration channels (Di Pietro *et al*, 2010) Loosely bound nuclei have been included in nuclear reactions, direct reactions occur at greater energy in general.

The direct reaction encompasses a wide range of nuclear reactions. Elastic scattering is the most basic direct reaction, maintaining the target nucleus in its ground state. When a projectile collides with a target nucleus and provides it several of its energy, it puts it to an active state, which is known as inelastic scattering. The energy of the active state is calculated by measuring the wasted energy (Nigussie, 2012).

In this study, we present our calculations explaining the elastic scattering and confined obtainable data for the weakly bound nucleus (unstable)  ${}^6\text{He}$  interacting with the heavy-mass  ${}^{208}\text{Pb}$ , and (stable)  ${}^7\text{Be}$  and  ${}^7\text{Li}$  interacting with the medium-mass  ${}^{58}\text{Ni}$  and  ${}^{59}\text{Co}$  respectively.

### Theoretical Background

The optical potential is composed of two components: the nuclear portion  $V_N$ , which is well and appropriately characterized by the Woods Saxon form, which has real and imaginary portions, and the Woods Saxon form, which is described by (Rehm, 1991):

$$V_N(r) = \frac{-V_0}{1+e^{(r-R_0)/a_0}} \quad (1)$$

where  $V_0$  is the potential depth,  $a$  is the surface diffuseness parameter, where  $r$  is the center of mass

distance between the target nucleus and the projectile nucleus and  $R_0$  is described by (Wang *et al*, 2009).

$$R_0 = r_0(\sqrt[3]{A_P} + \sqrt[3]{A_T}) \quad (2)$$

which is the system's radius,  $A_T$  the mass number of target nucleus and  $A_P$  the mass number of projectile nucleus.

Between the projectile and the target, there is an effective potential that separates them by the relative distance  $r$  as a function of the center of mass. It is divided into two parts, each of which is described below by (Timmers *et al*, 1995):

$$V_{\text{eff}}(r) = V_N(r) + V_C(r) \quad (3)$$

For the complete wave function, the Schrodinger equation would be (Piasecki *et al*, 2002):

$$\left( -\frac{\hbar^2}{2\mu} \nabla^2 + V_{\text{eff}}(r) + H_0(\xi) + V_{\text{coup}}(\xi) \right) \psi(\vec{r}, \xi) = E\psi(\vec{r}, \xi) \quad (4)$$

where  $r$  denotes the center of mass distance between accidental contact nuclei, and  $V(r)$  denotes the naked potential in the absence of coupling, where  $V_{\text{eff}}(r) = V_N(r) + V_C(r)$ ,  $H_0(\xi)$  denotes the Hamiltonian for intrinsic motion,  $V_{\text{coup}}(\xi)$  denotes the noted coupling, and  $\psi(\vec{r}, \xi)$  denotes the complete wave equation would be chosen to give by  $\vec{r}$  and  $\xi$ , where  $\xi$  is internal degree of freedom. we can write the rate of elastic differential cross section by using equation (Zagrebaev, 2008):

$$\frac{d\sigma_{el}}{d\sigma_R}(E, \theta) = \sum_{J\ell I} \frac{k_{nl}}{k} \left| \frac{f_{J\ell I}(E, \theta)}{f_C(E, \theta)} \right|^2 \quad (5)$$

where  $f_C(E, \theta)$  is the Coulomb scattering amplitude and  $f_{J\ell I}(E, \theta)$  elastic scattering amplitude.

### Results and Discussion

Figure 1 (A) shows the total differential cross section of scattering as a function of angle center of mass to the cross section of Rutherford  $\sigma_T/\sigma_R$  was determined with angle center of mass  $\theta_{cm}$  for the  ${}^6\text{He}+{}^{208}\text{Pb}$  system, the differential cross section of elastic scattering to the differential cross section of Rutherford  $\sigma_{el}/\sigma_R$  was calculated with energy center of mass  $E_{cm}$  in Figure 1 (B). The elastic scattering barrier distribution  $D_{el}$  was calculated with energy center of mass  $E_{cm}$  in figure 1 (C). The calculations have been performed for the nuclear system  ${}^6\text{He}+{}^{208}\text{Pb}$  where the projectile  ${}^6\text{He}$  is two neutron halo nucleus and the target  ${}^{208}\text{Pb}$  is heavy ion, using CDCC method and CC code for all order coupling channels with Akyüz-Winther potential parameters  $V_0 = 80.0$  MeV,  $a_0 = 0.63$  fm, and  $r_0 = 1.2$ fm, which are listed in Table 1. The best fitting between theoretical predictions and the



measured data was in case of coupled channels for all calculation of this system.

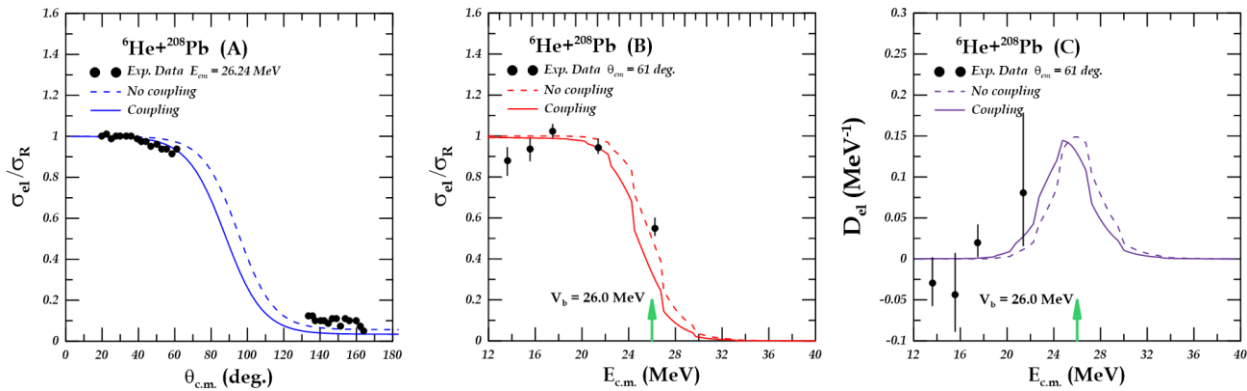


**Figure 1.** Uncoupled channel and coupled channels calculations for  ${}^6\text{He}+{}^{208}\text{Pb}$  system by dashed and solid curves respectively: Panel (A) elastic scattering differential cross section with the mass angle center, panel (B) scattering of elastic differential energy center of mass cross section, and panel (C) elastic scattering barrier distribution with the energy center of mass, the black circles act experimental data from Ref. (Fernández-García Alvarez *et al*, 2010)

In  ${}^7\text{Be}+{}^{58}\text{Ni}$  system, the elastic and total differential cross sections vary as a function of the angle center of mass. to the Rutherford differential cross section  $d\sigma_T / (d\sigma_R)$  was determined with angle center of mass  $\theta_{cm}$  in figure 2 (A), energy center of mass  $E_{cm}$  in figure 2 (B). The elastic scattering barrier distribution  $D_{el}$  was calculated with energy center of mass  $E_{cm}$  in figure 2 (C). The calculations have been performed for the nuclear system  ${}^7\text{Be}+{}^{58}\text{Ni}$  where

the projectile  ${}^7\text{Be}$  is weakly bound light nucleus and the target  ${}^{58}\text{Ni}$ , using CDCC method and CC code for all order coupling channels with Akyüz-Winther potential parameters  $V_0 = 50.6 \text{ MeV}$ ,  $a_0 = 0.63 \text{ fm}$ , and  $r_0 = 1.2 \text{ fm}$ , which are listed in Table 1. In the case of coupled channels, the excellent match between theoretical calculations and experimental data was for all calculations of this method.

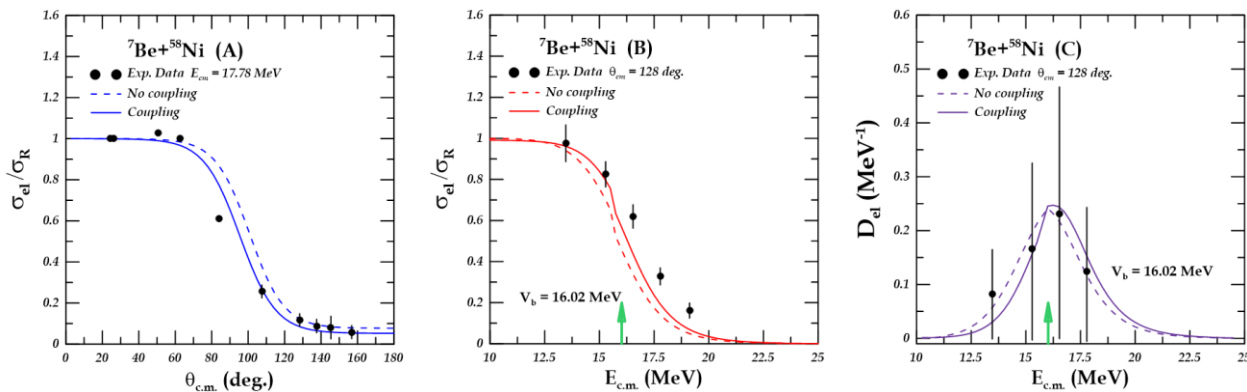


**Figure 2.** Uncoupled channel and coupled channels calculations for  ${}^7\text{Be}+{}^{58}\text{Ni}$  system by dashed and solid curves respectively: Panel (A) elastic scattering differential cross section with the mass angle center, panel (B) differential cross section of elastic scattering with energy center of mass, and panel (C) elastic scattering barrier distribution with the energy center of mass, the black circles act experimental data from Ref. (Beck *et al*, 2010).

In the  ${}^7\text{Li}+{}^{59}\text{Co}$  system, the results of this reaction are taken comparing the Rutherford differential cross section to the elastic differential cross section  $d\sigma_{el} / (d\sigma_R)$  was determined with angle center of mass  $\theta_{cm}$  (in figure 3, panel A), energy center of mass  $E_{cm}$  in figure 3 (B). The elastic scattering barrier distribution  $D_{el}$  was calculated with energy center of mass  $E_{cm}$  in figure 3 (C). The calculations have been performed for the nuclear system

${}^7\text{Li}+{}^{59}\text{Co}$  where the projectile  ${}^7\text{Li}$  is weakly bound light nucleus and the target  ${}^{59}\text{Co}$ , using CDCC method and CC code for all order coupling channels with Akyüz-Winther potential parameters  $V_0 = 51.4 \text{ MeV}$ ,  $a_0 = 0.63 \text{ fm}$ , and  $r_0 = 1.2 \text{ fm}$ , which are listed in Table 1. A good agreement between theoretical calculations and experimental data down Coulomb barrier in coupled and uncoupled calculations.



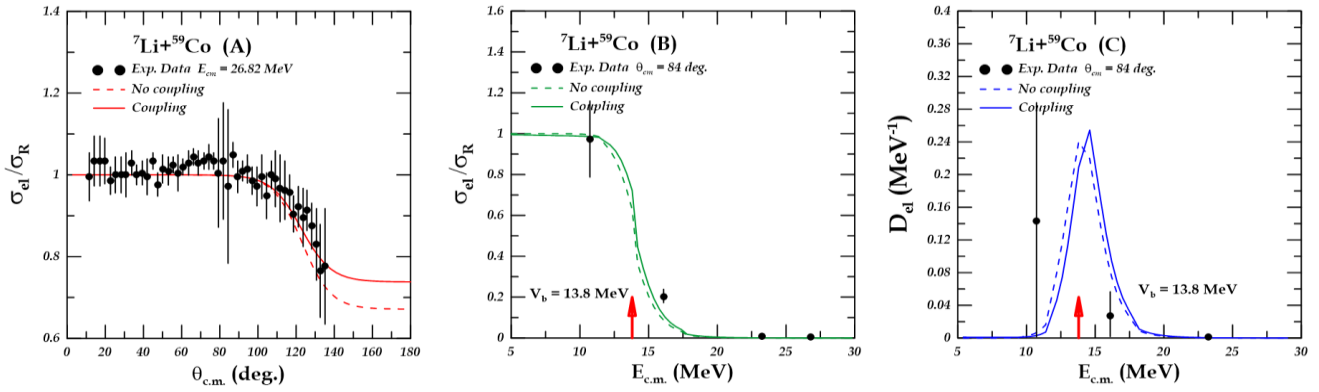


**Figure 3.** Uncoupled channel and coupled channels calculations for  ${}^7\text{Li}+{}^{59}\text{Co}$  system by dashed and solid curves respectively: Panel (A) elastic scattering differential cross section with the mass angle center, panel (B) differential cross section of elastic scattering with energy center of mass, and panel (C) elastic scattering barrier distribution with the energy center of mass, the black circles act experimental data from Ref. (Beck *et al*, 2007)

**Table 1.** Akyüz-Winther potential parameters, energy and scattering angle center of mass for  ${}^6\text{He}+{}^{208}\text{Pb}$ ,  ${}^7\text{Be}+{}^{58}\text{Ni}$  and  ${}^7\text{Li}+{}^{59}\text{Co}$  nuclear reactions

System	$V_0$ (MeV)	$r_0$ (fm)	$a_0$ (fm)	$W_i$ (MeV)	$r_i$ (fm)	$a_i$ (fm)	$V_b$ (MeV)	$E_{c.m.}$ (MeV)	$\theta_{c.m.}$ (deg)
${}^6\text{He}+{}^{208}\text{Pb}$	80.0	1.2	0.63	46.7	1.35	0.78	26.00	21.38	61
${}^7\text{Be}+{}^{58}\text{Ni}$	50.6	1.2	0.63	16.9	1.35	0.62	16.02	17.78	128
${}^7\text{Li}+{}^{59}\text{Co}$	51.4	1.2	0.63	17.1	1.35	0.48	13.80	10.72	84

### Conclusions

In elastic scattering, the effects of breakup coupling on  ${}^6\text{He}+{}^{208}\text{Pb}$ ,  ${}^7\text{Be}+{}^{58}\text{Ni}$  and  ${}^7\text{Li}+{}^{59}\text{Co}$  systems were implemented using the continuum discretized coupled channel (CDCC) approach. We examine angular distributions for a variety of collision energies and show that our theoretical results are quite close to current observations. We show that the nuclear excitations in target nucleus have a weakly effect on the elastic scattering, but that continuum-continuum couplings are required to generate the observations effects of coupled channels and breakup channels on calculations of elastic scattering have been studied using Code CC for weakly and exotic bound systems obtained through coupled-channels calculations. The method used in the present study can be considered as competitive method to study elastic scattering which is very important for study of elastic scattering.

### References

Back, B.B., Esbensen, H., Jiang, C.L., & Rehm, K.E. (2014). Recent developments in heavy-ion fusion reactions. *Reviews of Modern Physics*, 86(1), 317.  
 Bass, R. (1980). Fusion reactions: successes and limitations of a one-dimensional description. In *Deep-Inelastic and Fusion Reactions with Heavy Ions*, 281-293.  
 Beck C., Rowley N., Papka P., Courtin S., Rousseau M., Souza F.A., Carlin N., Liguori Neto R., de Moura M.M., Del Santo M.G., Suaide A.A.P., Munhoz M.G., Szanto E.M., Szanto de Toledo A,

Keeley N., Diaz-Torres A., Hagino K. (2010). Reaction mechanisms for weakly-bound, stable nuclei and unstable, halo nuclei on medium-mass targets. *Nuclear Physics A* 834(1-4), 440c-445c.  
 Beck, C., Keeley, N., & Diaz-Torres, A. (2007). Coupled-channel effects in elastic scattering and near-barrier fusion induced by weakly bound nuclei and exotic halo nuclei. *Physical Review C*, 75(5), 054605.  
 Berkdemir, C., Berkdemir, A., & Sever, R. (2005). Polynomial solutions of the Schrödinger equation for the generalized Woods-Saxon potential. *Physical Review C*, 72(2), 027001.  
 Canto, L.F., Gomes, P. R. S., Donangelo, R., & Hussein, M.S. (2006). Fusion and breakup of weakly bound nuclei. *Physics reports*, 424(1-2), 1-111.  
 Canto, L.F., Gomes, P.R.S., Donangelo, R., Lubian, J., & Hussein, M.S. (2015). Recent developments in fusion and direct reactions with weakly bound nuclei. *Physics Reports*, 596, 1-86.  
 Denisov, V.Y. (2004, April). Superheavy element production, nucleus-nucleus potential and  $\mu$ -catalysis. In *AIP Conference Proceedings*, 704(1), 92-101.  
 Denisov, V.Y., & Nesterov, V.A. (2006). Distribution of density and potential of nuclear interaction. *Ukrayins' kij Fydzichnij Zhurnal (Kiev)*, 51(5), 440-448.  
 Di Pietro A., Randisi G., Scuderi V., Acosta L., Amorini F., Borge M.J.G., Figuera P., Fisichella M., Fraile L. M., Gomez-Camacho J., Jeppesen H., Lattuada M., Martel I., Milin M., Musumarra A., Papa M., Pellegriti M. G., Perez-Bernal F., Raabe R., Rizzo F., Santonocito D., Scalia G., Tengblad O., Torresi D., Maira Vidal A., Voulot D., Wenander F., & Zadro M. (2010). Elastic scattering and reaction mechanisms of the halo nucleus Be 11 around the Coulomb barrier. *Physical review letters* 105(2), 022701.  
 Fernández-García, J.P., Alvarez, M.A.G., Moro, A.M., & Rodríguez-Gallardo, M. (2010). Simultaneous analysis of elastic scattering and transfer/breakup channels for the  ${}^6\text{He}+$



- 208Pb reaction at energies near the Coulomb barrier. *Physics Letters B* 693(3), 310-315.
- Gasques, L.R., Evers, M., Hinde, D.J., Dasgupta, M., Gomes, P.R.S., Anjos, R.M., & Hagino, K. (2007). Systematic study of the nuclear potential through high precision back-angle quasi-elastic scattering measurements. *Physical Review C*, 76(2).
- Hagino, K. (2007). Recent developments in quasi-elastic scattering around the Coulomb barrier. In *AIP Conference Proceedings*, 891(1), 80-88.
- Hagino, K., & Watanabe, Y. (2007). Potential inversion with sub-barrier fusion data reexamined. *Physical Review C*, 76(2).
- Hagino, K., Takehi, T., Balantekin, A.B., & Takigawa, N. (2005). Surface diffuseness anomaly in heavy-ion potentials for large-angle quasielastic scattering. *Physical Review C*, 71(4).
- Ibrahim, M.I., Zamrun, M., & Kassim, H.A. (2013). Analysis of the nuclear potential for heavy-ion systems through large-angle quasi-elastic scattering. *Physical Review C*, 87(2), 024611.
- Keeley, N., Alamanos, N., Kemper, K.W., & Rusek, K. (2009). Elastic scattering and reactions of light exotic beams. *Progress in Particle and Nuclear Physics*, 63(2), 396-447.
- Keeley, N., Raabe, R., Alamanos, N., & Sida, J. L. (2007). Fusion and direct reactions of halo nuclei at energies around the Coulomb barrier. *Progress in Particle and Nuclear Physics*, 59(2), 579-630.
- Nigussie, B. (2012). *Complete and incomplete fusion studies in some  $14N+ {}^{59}\text{Co}$  systems* (Doctoral dissertation, Addis Ababa University).
- Pahlavani, M.R., Sadeghi, J., & Ghezelbash, M. (2009). Solutions of the central Woods-Saxon potential in case using mathematical modification method. *APPS. Applied Sciences*, 11, 106-113.
- Piasecki, E.; Kowalczyk, M.; Piasecki, K.; Świdorski, Ł.; Srebrny, J.; Witecki, M.; Carstoiu, F.; Czarnacki, W.; Rusek, K.; Iwanicki, J.; Jastrzębski, J.; Kisieliński, M.; Kordyasz, A.; Stolarz, A.; Tys, J.; Krogulski, T.; Rowley, N. (2002). Barrier distributions in  $160+116$ ,  $119\text{Sn}$  quasielastic scattering. *Physical Review C* 65(5).
- Rehm, K.E. (1991). Quasi-elastic heavy-ion collisions. *Annual Review of Nuclear and Particle Science*, 41(1), 429-468.
- Satchler, G.R. (1983). *Nuclear Direct Reactions*, Clarendon.
- Tanihata, I. (1996). Neutron halo nuclei. *Journal of Physics G: Nuclear and Particle Physics*, 22(2).
- Timmers H., Leigh J.R., Dasgupta M., Hinde D.J., Lemmon R.C., Mein J.C., Morton C.R., Newton J.O., Rowley N. (1995). Probing fusion barrier distributions with quasi-elastic scattering. *Nuclear Physics A* 584(1), 190-204.
- Wang, N., Liu, M., & Yang, Y. (2009). Heavy-ion fusion and scattering with Skyrme energy density functional. *Science in China Series G: Physics, Mechanics and Astronomy*, 52(10), 1554-1573.
- Washiyama, K., Hagino, K., & Dasgupta, M. (2006). Probing surface diffuseness of nucleus-nucleus potential with quasielastic scattering at deep sub-barrier energies. *Physical Review C*, 73(3).
- Wong, C. (1973). Interaction barrier in charged-particle nuclear reactions. *Physical Review Letters*, 31(12).
- Zagrebaev, V.I. (2008). Understanding the barrier distribution function derived from backward-angle quasi-elastic scattering. *Physical Review C*, 78(4).

